Supporting information

Taylor Dispersion Analysis and Atomic Force Microscopy provide quantitative insight on the aggregation kinetics of Aβ(1-40)/Aβ(1-42) amyloid peptide mixtures

*Mihai Deleanu[1], Olivier Deschaume[2], Luca Cipelletti[3,4], Jean-François Hernandez[1], Carmen Bartic[2], Hervé Cottet[*1], Joseph Chamieh[*1]*

[1]IBMM, Univ Montpellier, CNRS, ENSCM, Montpellier, France

[2]Department of Physics and Astronomy, Soft-Matter Physics and Biophysics Section, KU Leuven, Celestijnenlaan 200D, Box 2416, 3001 Heverlee, Belgium

[3]L2C, Université Montpellier, 34095 Montpellier, France

[4]Institut Universitaire de France (IUF), France

[*] CORRESPONDING AUTHOR

Tel: +33 4 6714 3920, Fax: +33 4 6763 1046. E-mail: joseph.chamieh@umontpellier.fr

Tel: +33 4 6714 3427, Fax: +33 4 6763 1046. E-mail: herve.cottet@umontpellier.fr

Table of contents

1. TDA: Theory and data processing

Conditions for TDA validity. The band broadening resulting from Taylor dispersion is easily quantified via the temporal variance of the elution profile. The diffusion coefficient D ($m^2\ s^{-1}$) and the hydrodynamic radius R_h (m) are determined using Eq. (1) and Eq. (2), respectively:

$$D = \frac{R_c^2 t_0}{24\sigma^2} \quad \text{SI.(1)}$$

$$R_h = \frac{k_b T}{6\pi\eta D} \quad \text{SI.(2)}$$

where R_c is the capillary radius (m), t_0 is the average elution time (s), σ^2 is the temporal variance of the peak (s^2), k_B is the Boltzmann constant, T the temperature (K) and η the viscosity of the carrier liquid (Pa.s). It is noteworthy that Eq. (1) is valid when the peak appearance time t_0 is higher than the characteristic diffusion time of the solute over a distance equal to the capillary radius as verified by Eq. (3)[1, 2]:

$$\tau = \frac{D t_0}{R_c^2} \geq 1.25 \quad \text{SI.(3)}$$

where τ is an adimensional characteristic time. Axial diffusion should also be negligible compared to convection as verified by Eq. (4)[1, 2]:

$$P_e = \frac{u R_c}{D} \geq 40 \quad \text{SI.(4)}$$

where P_e is the Péclet number and u is the linear mobile phase velocity (m/s).

Data processing of the taylorgrams. The taylorgram *S(t)* of a sample mixture containing *n* different components of individual diffusion coefficient D_i can be expressed as a sum of *n* individual Gaussian contributions $S_i(t)$, all centered at the same elution time t_0:

$$S(t) = \sum_{i=1}^{n} S_i(t) = \sum_{i=1}^{n} \frac{A_i}{\sigma_i \sqrt{2\pi}} e^{-\frac{1}{2}\frac{(t-t_0)^2}{\sigma_i^2}} \qquad \text{SI.(5)}$$

where A_i is a coefficient that is proportional to the concentration in species *i* and depends on the response coefficient of the species *i,* at the specific detection wavelength. The diffusion coefficient of the species *i* is directly related to the standard deviation σ_i according to

$$D_i = \frac{R_c^2 t_0}{24\sigma_i^2} \qquad \text{SI.(6)}$$

Different approaches can be used to obtain information about the size distribution of the species in the mixture from the taylorgram *S(t)*.[3-5]

A first approach is based on a direct curve fitting with the sum of *n* Gaussian curves according to Eq. (5), when the total number of species, *n,* is limited ($n \leq 4$). The curve fitting was conducted using the Least Significant Difference method using the "GRG nonlinear" algorithm in Microsoft Excel.

A second approach is based on Constrained Regularized Linear Inversion (CRLI)[4] which aims at finding the probability density function $P_D(D)$ that fits the taylorgram according to the following equation:

$$s(t) = c\int_0^{\infty} P_D(D)\sqrt{D}\exp\left[-\frac{(t-t_0)^2 12D}{R_c^2 t_0}\right] dD \qquad \text{SI.(7)}$$

with $c = \left[\int_0^\infty P_D(D) \sqrt{D} dD \right]^{-1} = \left[\overline{D^{1/2}} \right]^{-1}$ a normalization factor and $P_D(D)$ the mass-weighted probability distribution function (PDF) of the diffusion coefficient. The main advantage of this approach, as compared to the first one, is that there is no need to hypothesize on the number of populations under the experimental distribution. For more details on that approach, the reader may refer to original publications [3, 4].

2. Experimental Taylorgrams

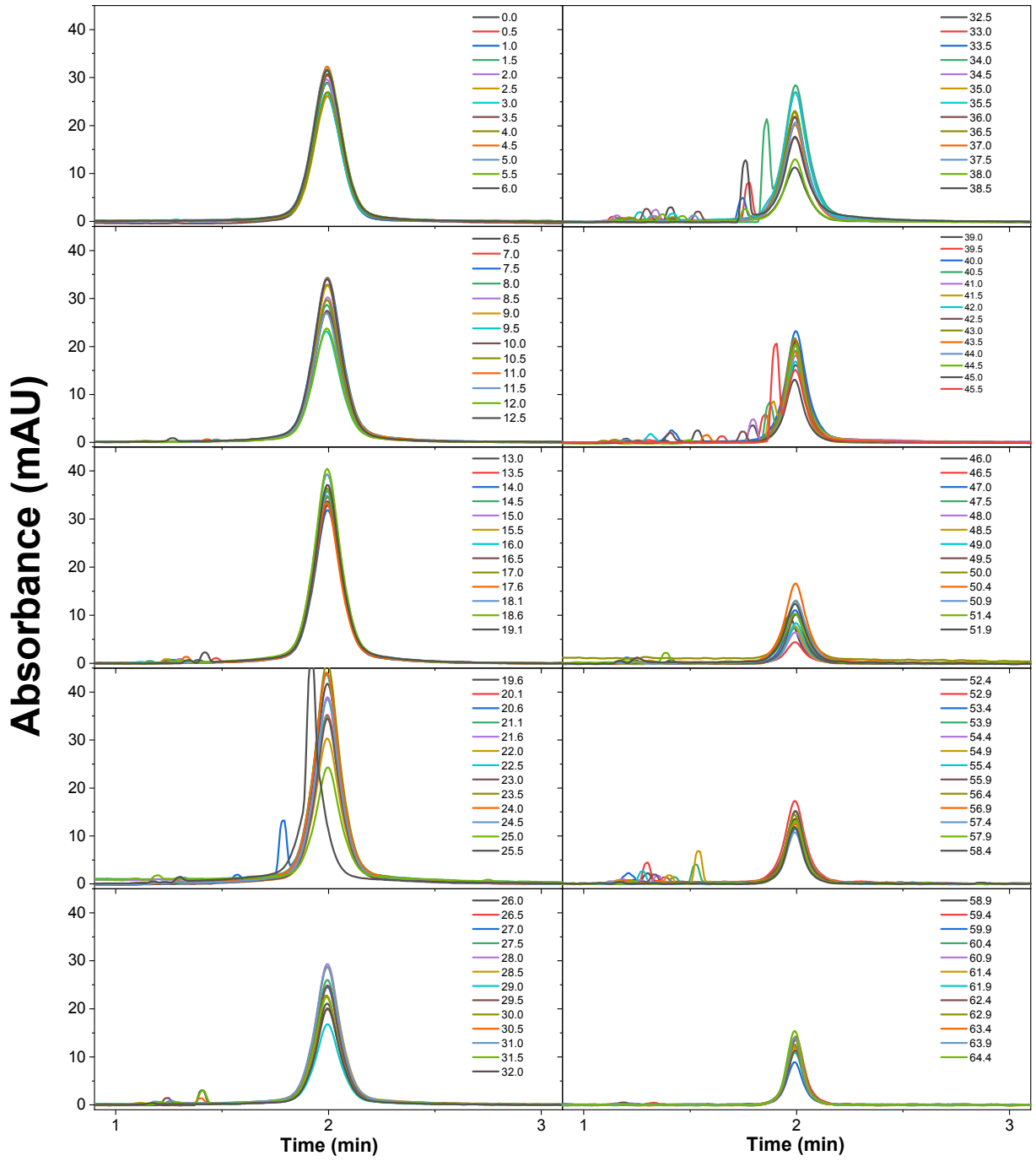

Figure SI.1. Experimental taylorgrams obtained for Aβ(1-40) aggregation monitoring over an incubation period of 65 h. The experimental traces are distributed into several graphs for better

clarity. Curves are colored with respect to incubation time, in h. Experimental conditions: Sample: 133 μM Aβ(1-40) in 20 mM phosphate buffer pH 7.4. Incubation: quiescent conditions at 37 ˚C. Fused silica capillary: 50 μm i.d. × 40 cm × 31.5 cm. Eluent: 20 mM phosphate buffer, pH 7.4. Mobilization pressure: 100 mbar. Injection: 44 mbar for 3 s (V_{inj} = 7 nL, corresponding to 1% of capillary volume to injection point). Analyses were performed at 37 ˚C. UV detection at 191 nm.

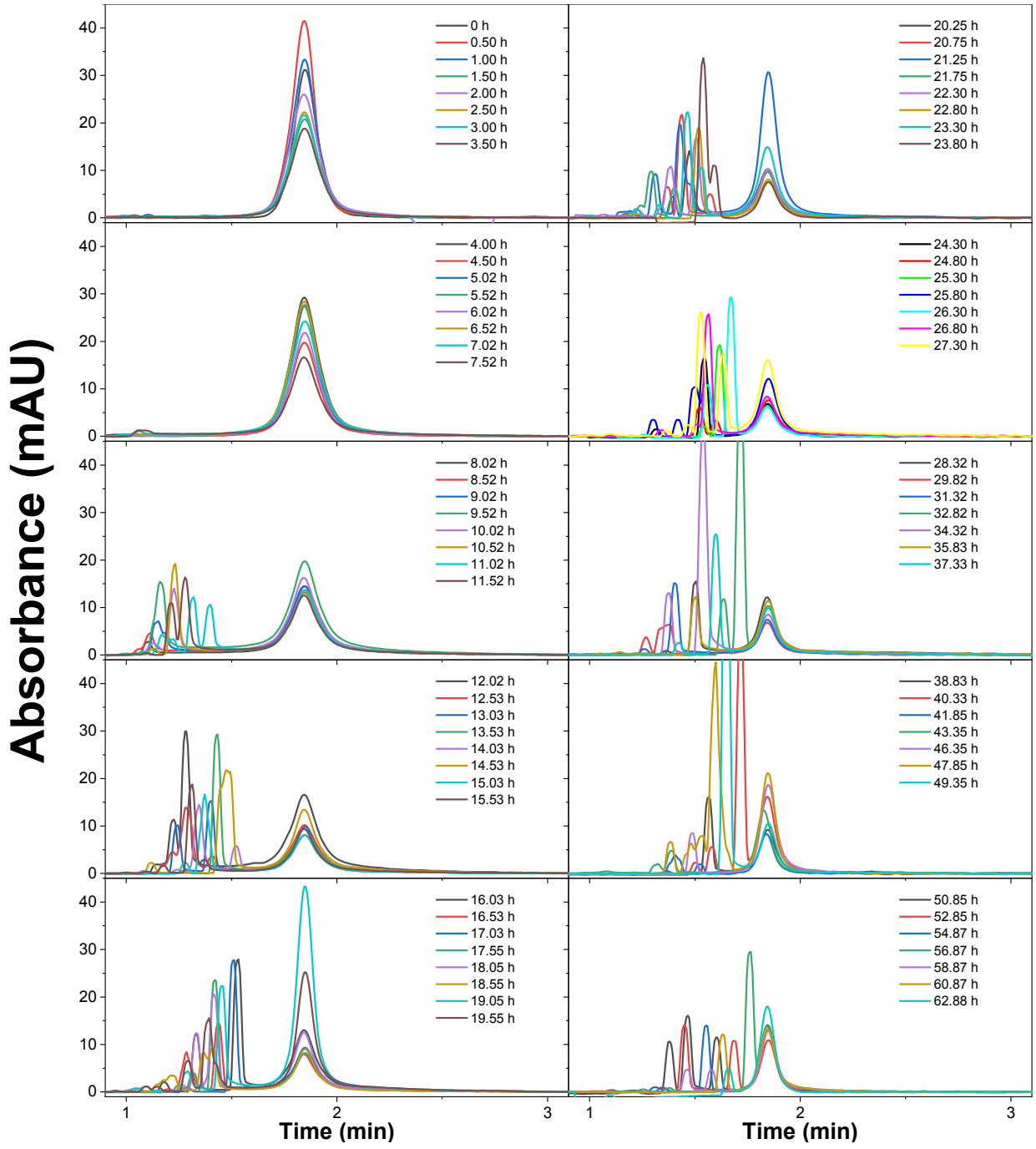

Figure SI.2. Experimental taylorgrams obtained for Aβ(1-40):Aβ(1-42) 3:1 mixture aggregation monitoring over an incubation period of 65 h. The experimental traces are distributed into several graphs for better clarity. Curves are colored with respect to incubation time, in h. Experimental

77 conditions: Sample: 100 μM of Aβ(1-40) and 33 μM Aβ(1-42) of in 20 mM phosphate buffer pH

78 7.4. Incubation: quiescent conditions at 37 ˚C. Fused silica capillary: 50 μm i.d. × 40 cm × 31.5

79 cm. Eluent: 20 mM phosphate buffer, pH 7.4. Mobilization pressure: 100 mbar. Injection: 44 mbar

80 for 3 s (V_{inj} = 7 nL, corresponding to 1% of capillary volume to injection point). Analyses were

81 performed at 37 ˚C. UV detection at 191 nm.

82

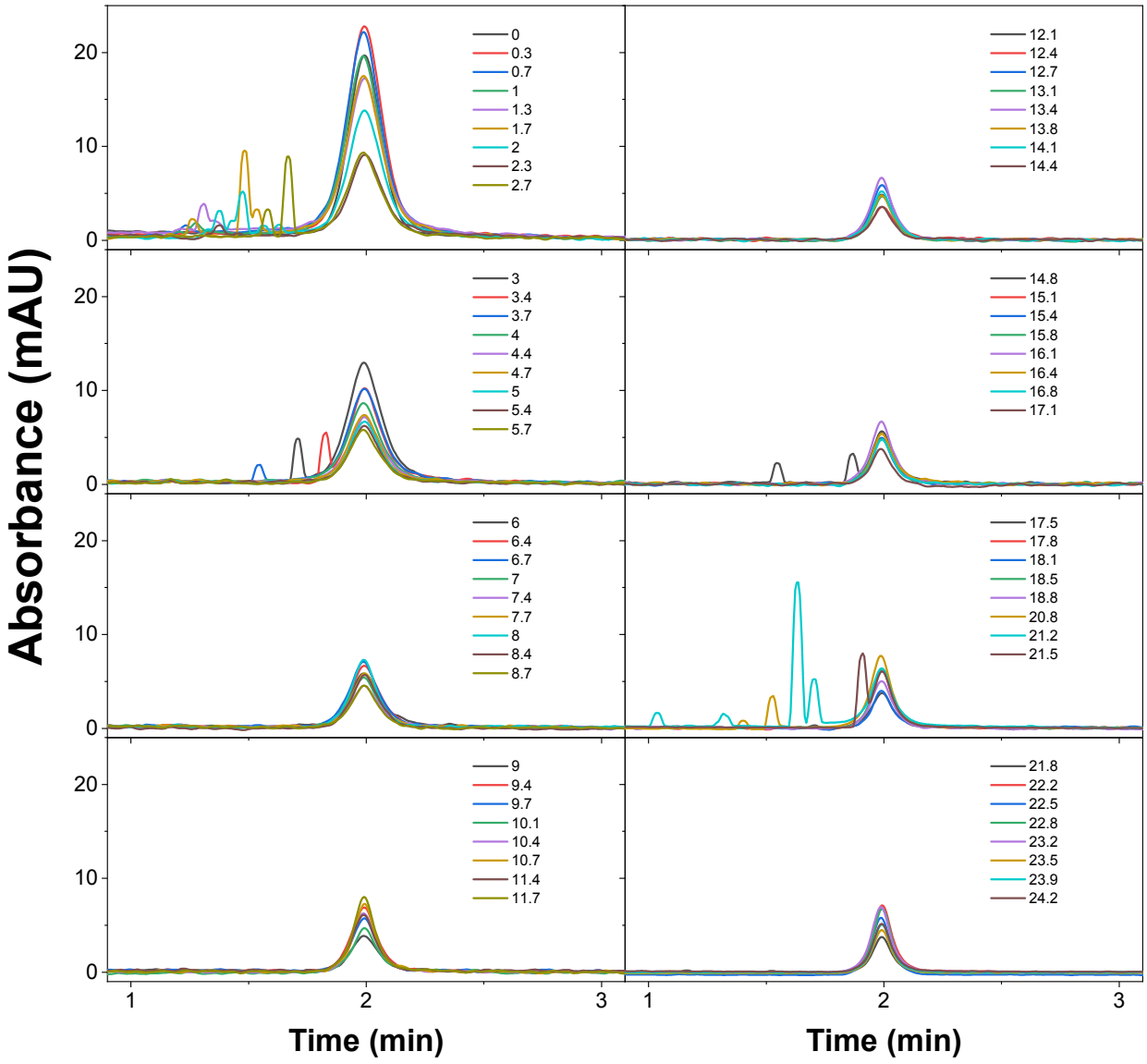

Figure SI.3. Experimental taylorgrams obtained for Aβ(1-40):Aβ(1-42) 1:1 mixture aggregation monitoring over an incubation period of 25 h. The experimental traces are distributed into several graphs for better clarity. Curves are colored with respect to incubation time, in h. Experimental conditions: Sample: 66.7 μM of Aβ(1-40) and 66.7 μM Aβ(1-42) of in 20 mM phosphate buffer pH 7.4. Incubation: quiescent conditions at 37 ˚C. Fused silica capillary: 50 μm i.d. × 40 cm × 31.5

89 cm. Eluent: 20 mM phosphate buffer, pH 7.4. Mobilization pressure: 100 mbar. Injection: 44 mbar

90 for 3 s (V_{inj} = 7 nL, corresponding to 1% of capillary volume to injection point). Analyses were

91 performed at 37 ˚C. UV detection at 191 nm.

92

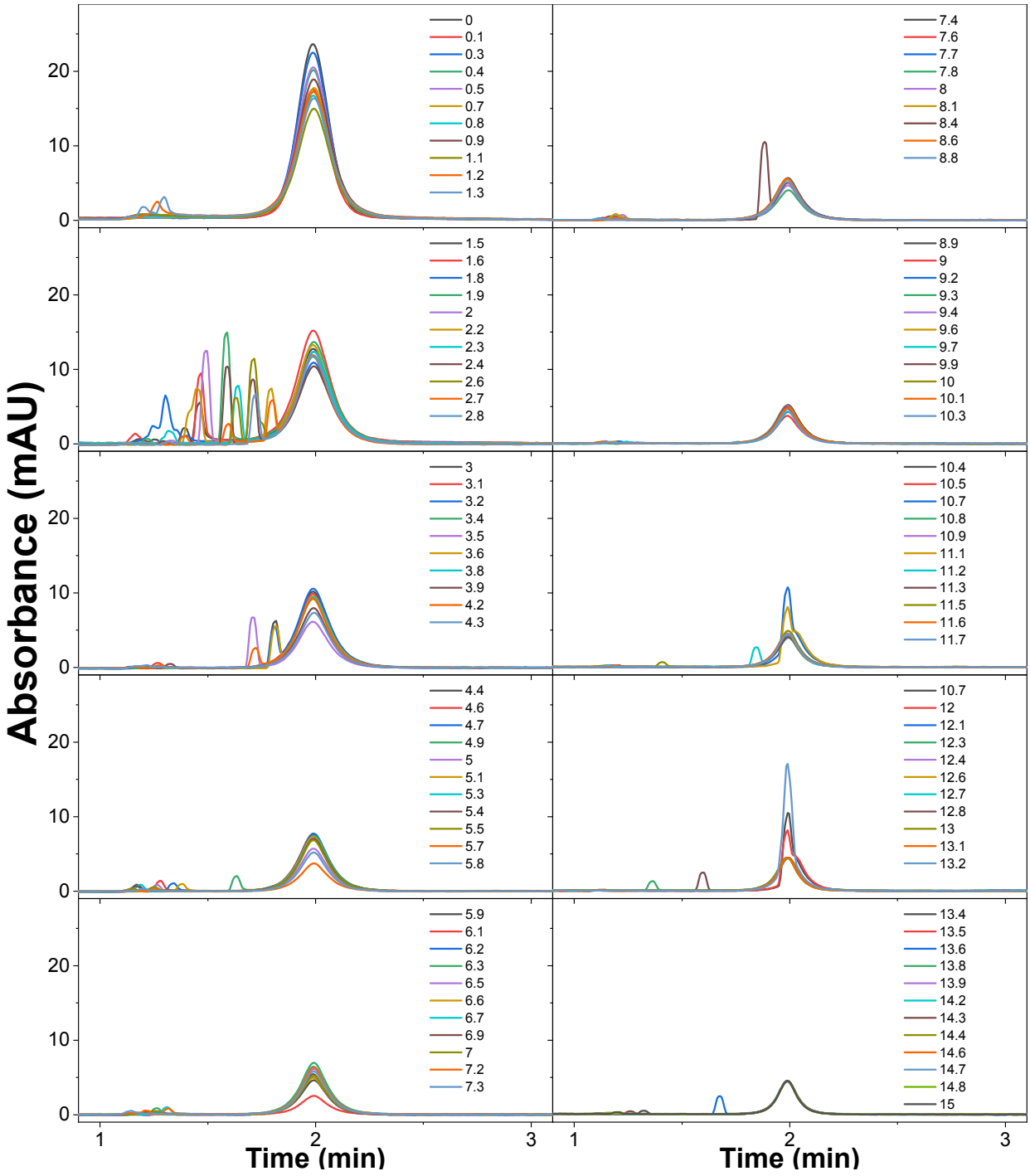

Figure SI.4. Experimental taylorgrams obtained for Aβ(1-40):Aβ(1-42) 1:3 mixture aggregation monitoring over an incubation period of 15 h. The experimental traces are distributed into several

graphs for better clarity. Curves are colored with respect to incubation time, in h. Experimental conditions: Sample: 33 µM of Aβ(1-40) and 100 µM Aβ(1-42) of in 20 mM phosphate buffer pH 7.4. Incubation: quiescent conditions at 37 ˚C. Fused silica capillary: 50 µm i.d. × 40 cm × 31.5 cm. Eluent: 20 mM phosphate buffer, pH 7.4. Mobilization pressure: 100 mbar. Injection: 44 mbar for 3 s (V_{inj} = 7 nL, corresponding to 1% of capillary volume to injection point). Analyses were performed at 37 ˚C. UV detection at 191 nm.

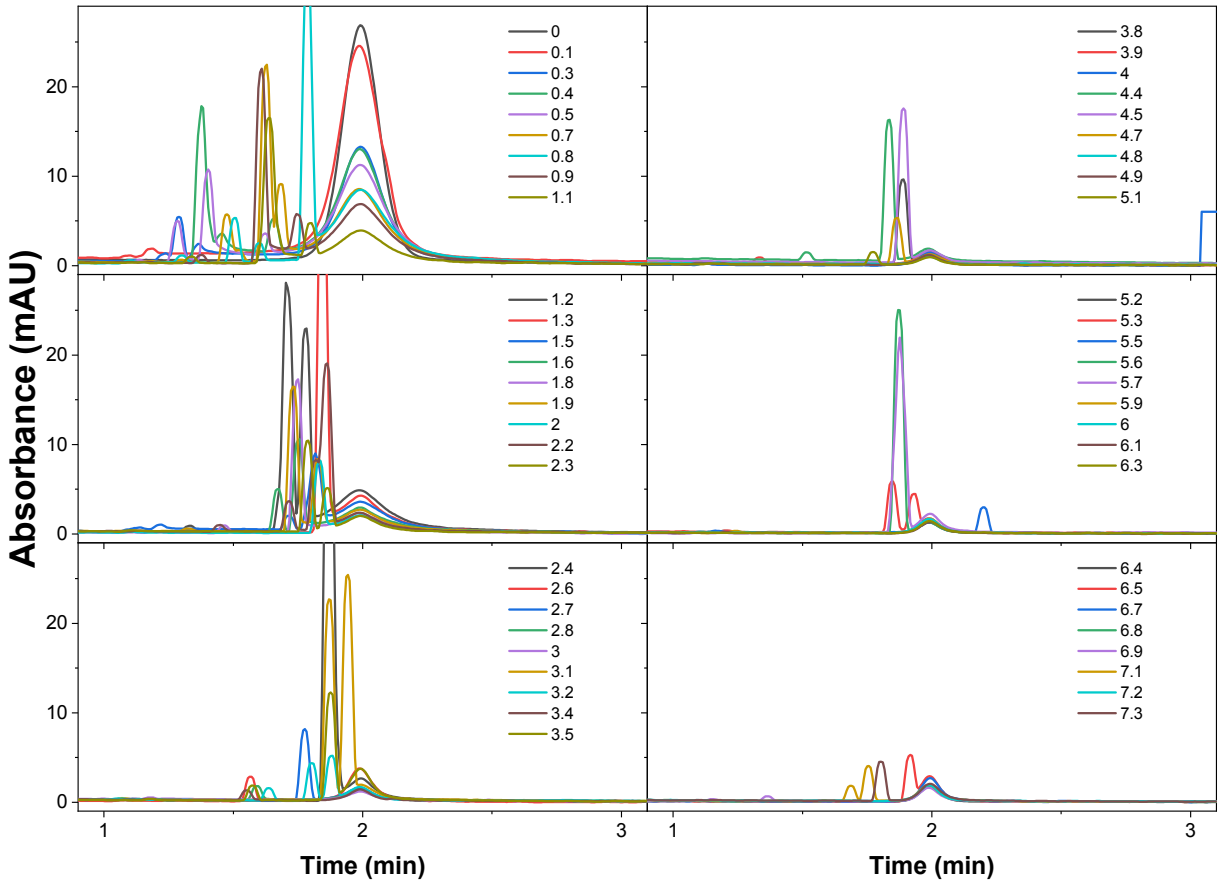

Figure SI.5. Experimental taylorgrams obtained for Aβ(1-42) aggregation monitoring over an incubation period of 8 h. The experimental traces are distributed into several graphs for better clarity. Curves are colored with respect to incubation time, in h. Experimental conditions: Sample: 133 µM Aβ(1-42) in 20 mM phosphate buffer pH 7.4. Incubation: quiescent conditions at 37 °C. Fused silica capillary: 50 µm i.d. × 40 cm × 31.5 cm. Eluent: 20 mM phosphate buffer, pH 7.4. Mobilization pressure: 100 mbar. Injection: 44 mbar for 3 s (V_{inj} = 7 nL, corresponding to 1% of capillary volume to injection point). Analyses were performed at 37 °C. UV detection at 191 nm.

3. Data treatment by Taylor dispersion analysis

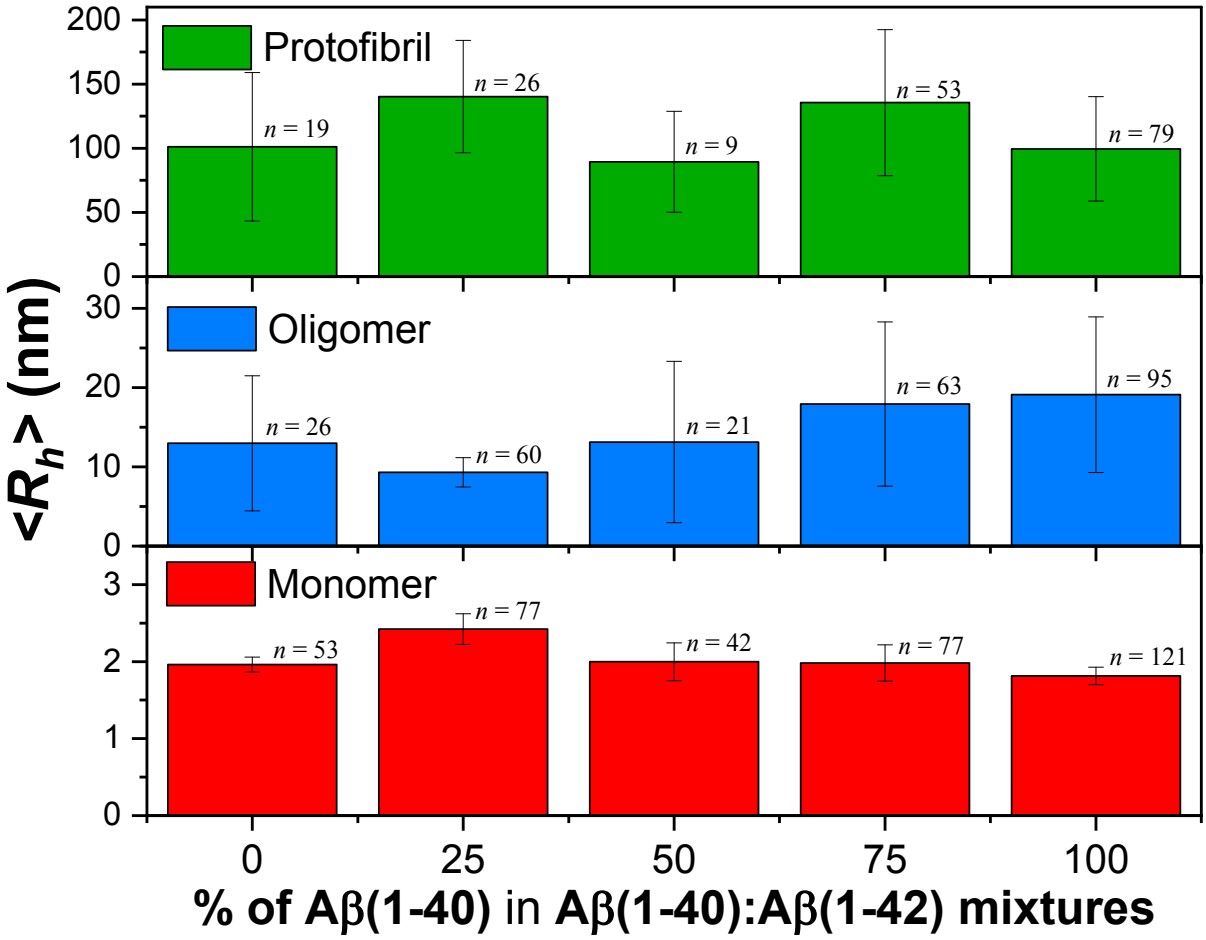

Figure SI.6. Average hydrodynamic radii for the monomer, oligomers and protofibrils size populations obtained by the deconvolution of the taylorgrams with a finite number of Gaussian functions and as a function of the % of Aβ(1-40) in Aβ(1-40):Aβ(1-42) mixtures. The error bars are standard deviations calculated on *n* repetitions as indicated in the figure.

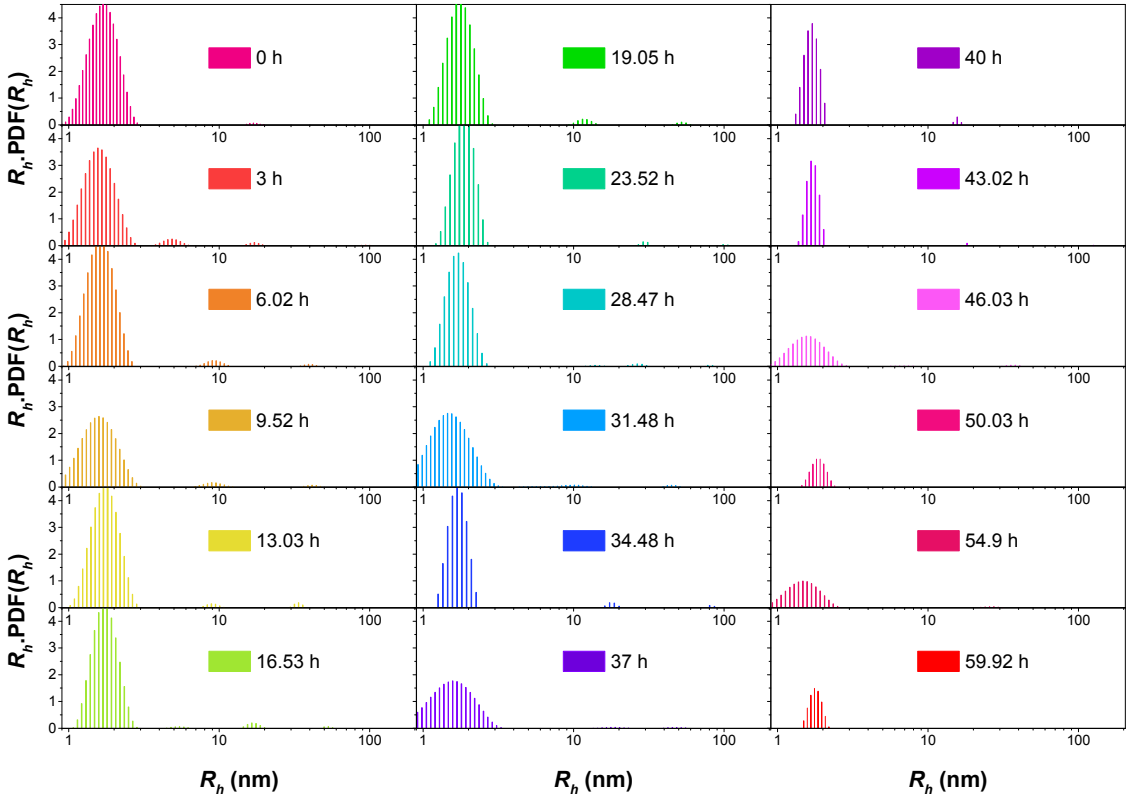

Figure SI.7. Size distributions of Aβ(1-40) (133.3 μM) obtained by CRLI analysis of the experimental taylorgrams as a function of incubation time t_{ag} = 0 to ~60 h. Experimental taylorgrams are shown in figure SI.1.

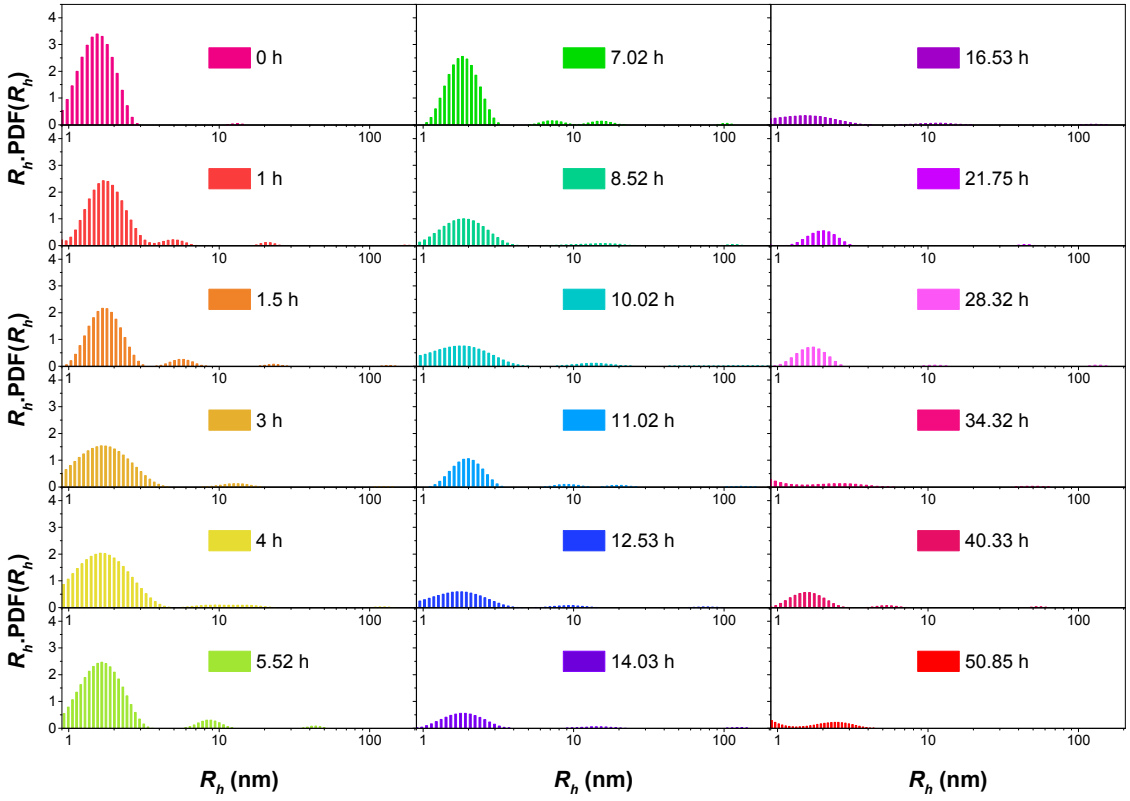

122

123 **Figure SI.8.** Size distributions of Aβ(1-40):Aβ(1-42) 3:1 mixture (100 μM and 33.3 μM
124 respectively) obtained by CRLI analysis of the experimental taylorgrams as a function of
125 incubation time t_{ag} = 0 to ~50 h. Experimental taylorgrams are shown in figure SI.2.

126

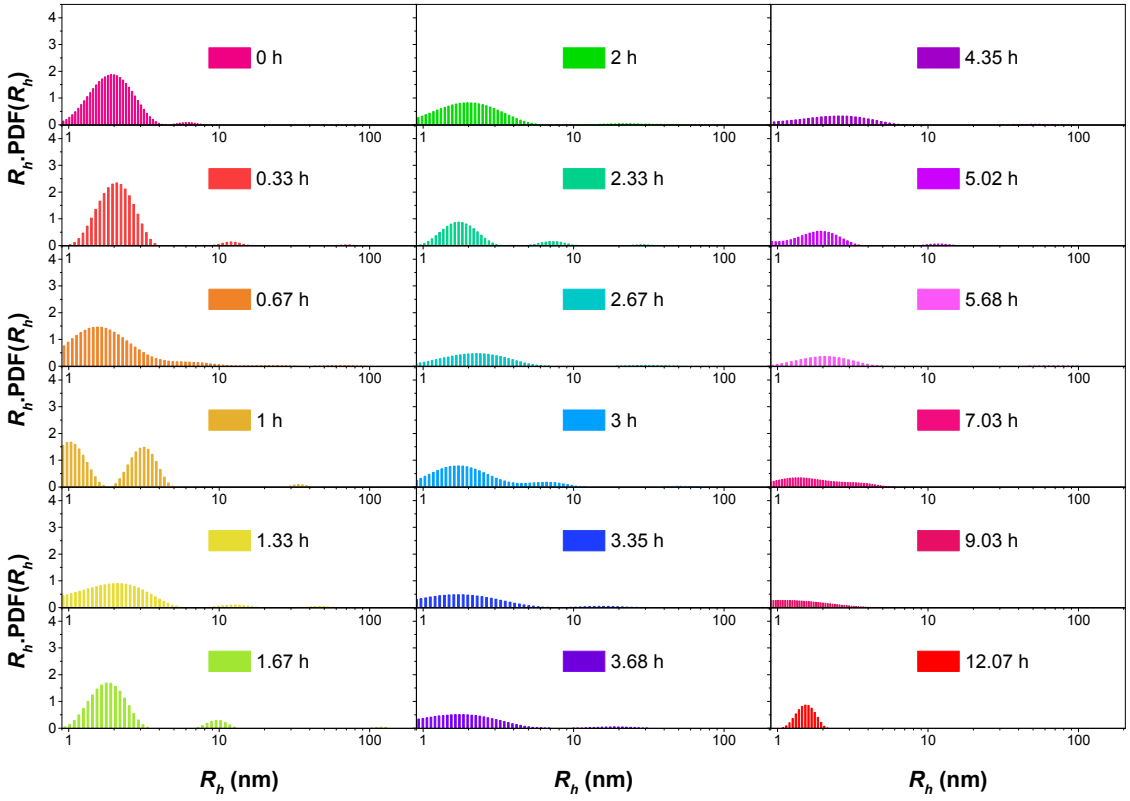

127

128 **Figure SI.9.** Size distributions of Aβ(1-40):Aβ(1-42) 1:1 mixture (66.7 μM and 66.7 μM
129 respectively) obtained by CRLI analysis of the experimental taylorgrams as a function of
130 incubation time t_{ag} = 0 to ~12 h. Experimental taylorgrams are shown in figure SI.3.

131

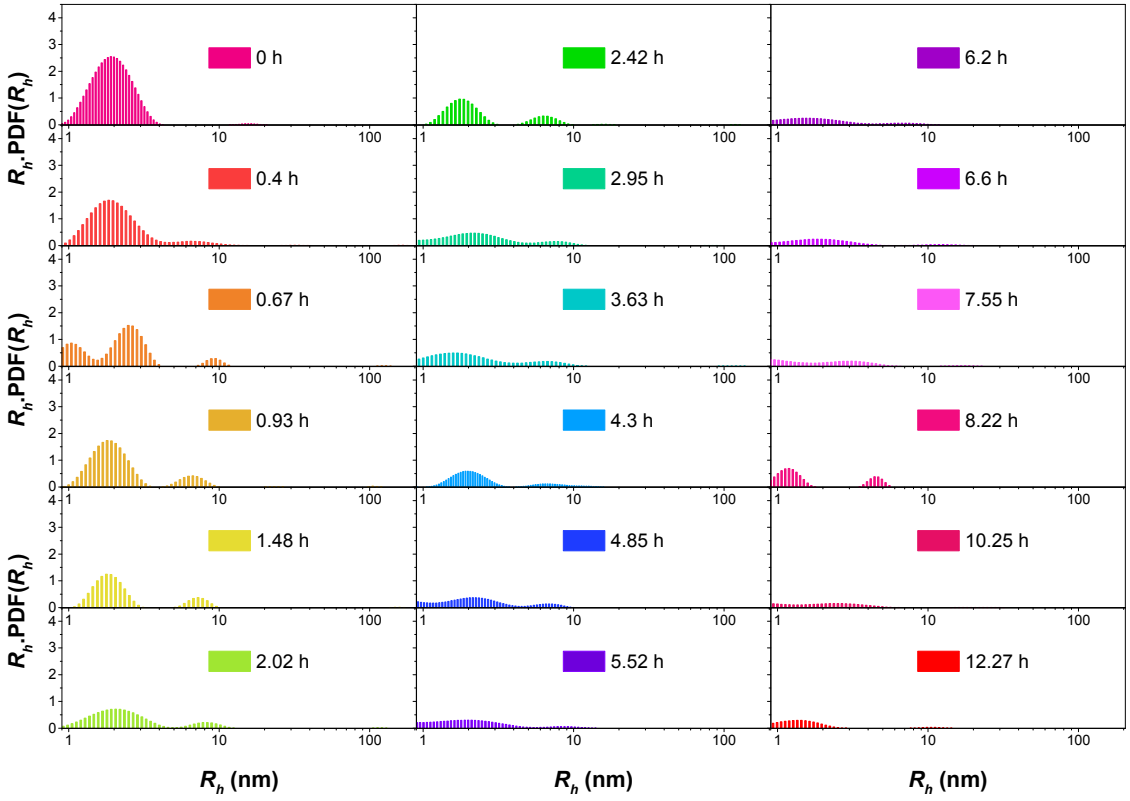

132

133 **Figure SI.10.** Size distributions of Aβ(1-40):Aβ(1-42) 1:3 mixture (33.3 μM and 100 μM
134 respectively) obtained by CRLI analysis of the experimental taylorgrams as a function of
135 incubation time t_{ag} = 0 to ~12 h. Experimental taylorgrams are shown in figure SI.4.

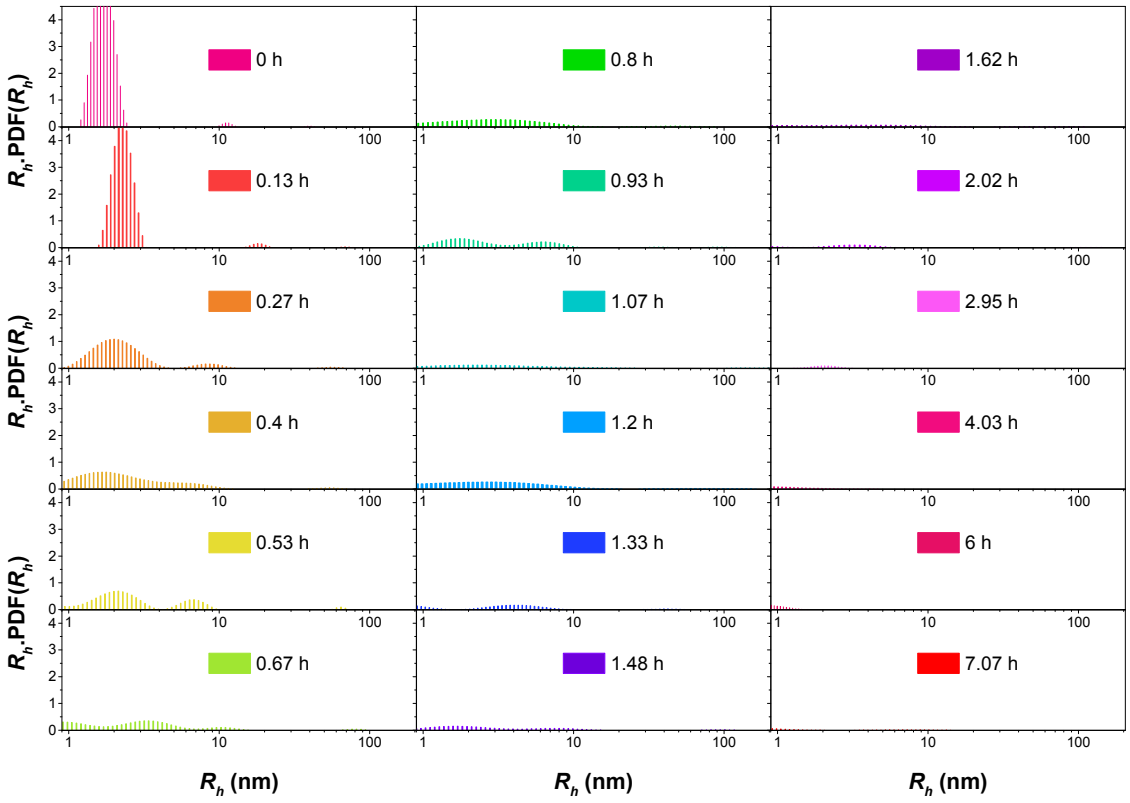

136

137 **Figure SI.11.** Size distributions of Aβ(1-42) (133.3 μM) obtained by CRLI analysis of the
138 experimental taylorgrams as a function of incubation time t_{ag} = 0 to ~7 h. Experimental
139 taylorgrams are shown in figure SI.5.

140

4. Kinetics of the aggregation process

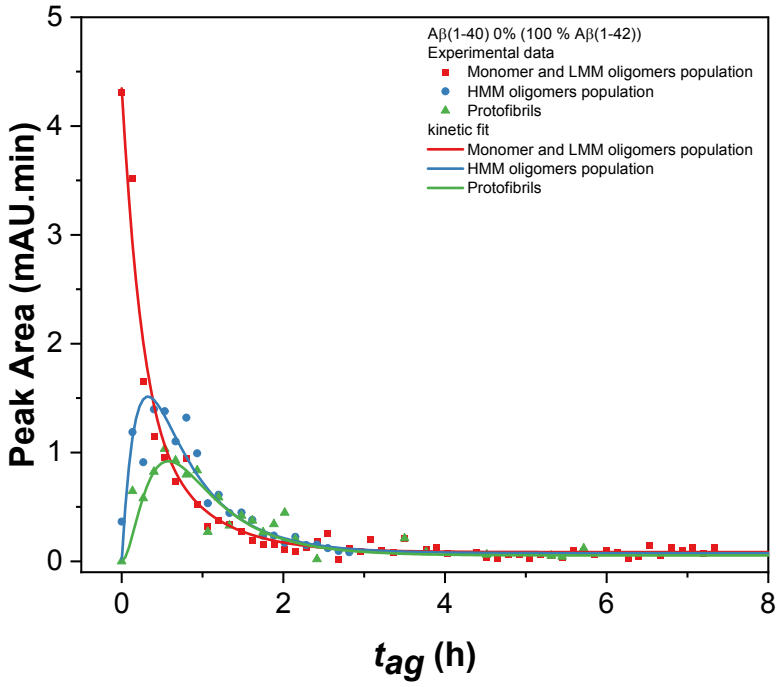

Figure SI.12. Symbols: time evolution of the peak area corresponding to the various populations obtained by deconvolution of the TDA signal for the Aβ(1-40) 0% sample. Lines: fits of the reaction kinetics, considering forward and backward reactions, Eqs. (5-7) in the main manuscript.

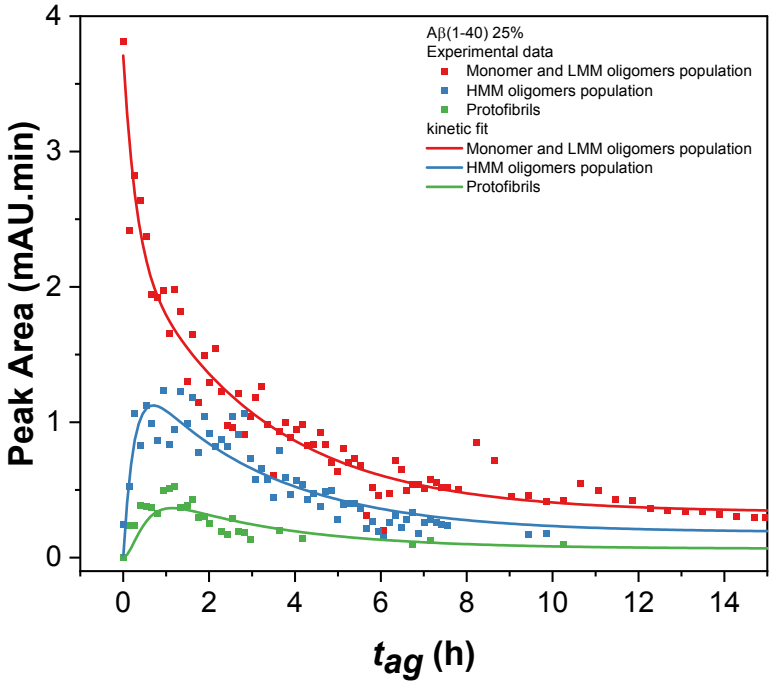

Figure SI.13. Symbols: time evolution of the peak area corresponding to the various populations obtained by deconvolution of the TDA signal for the Aβ(1-40) 25% sample. Lines: fits of the reaction kinetics, considering forward and backward reactions, Eqs. (5-7) in the main manuscript.

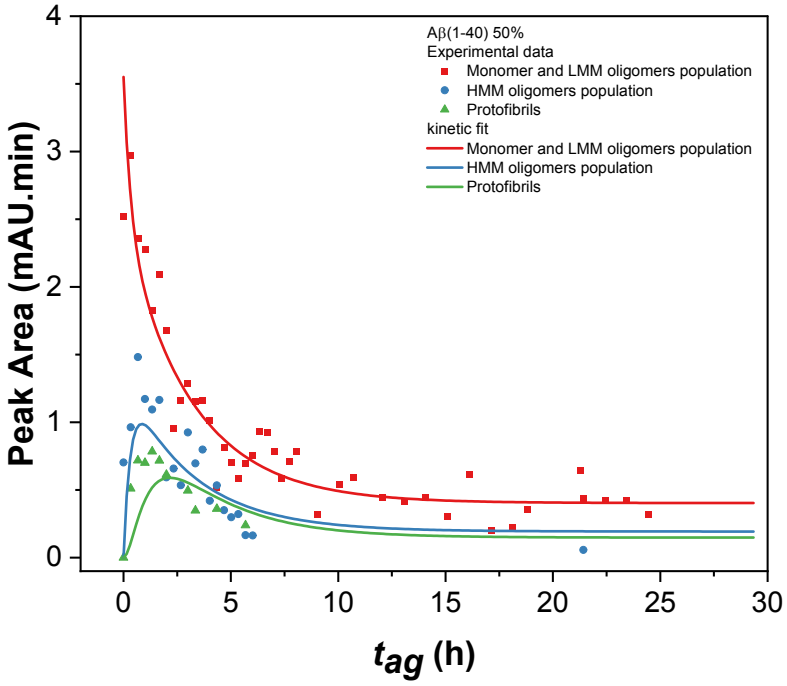

Figure SI.14. Symbols: time evolution of the peak area corresponding to the various populations obtained by deconvolution of the TDA signal for the Aβ(1-40) 50% sample. Lines: fits of the reaction kinetics, considering forward and backward reactions, Eqs. (5-7) in the main manuscript.

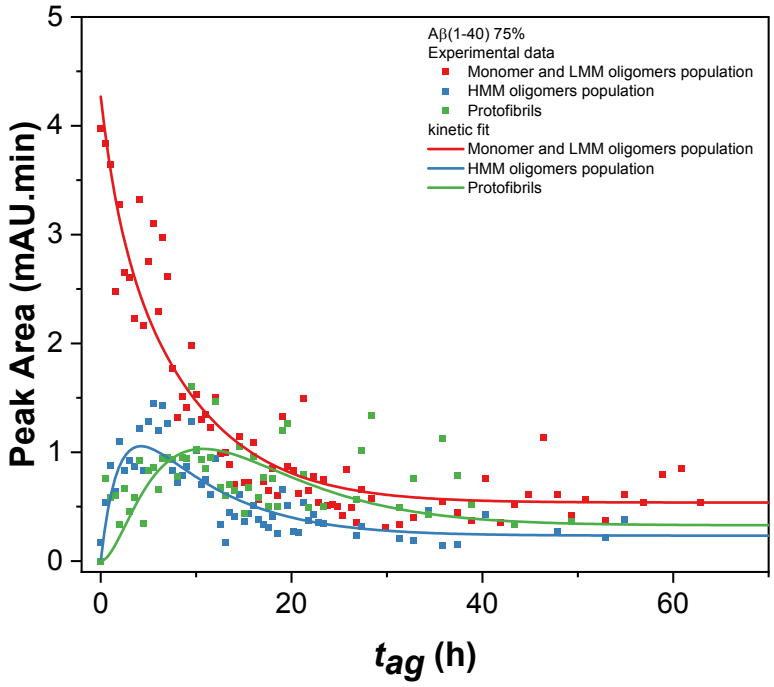

156

157 **Figure SI.15.** Symbols: time evolution of the peak area corresponding to the various populations
158 obtained by deconvolution of the TDA signal for the Aβ(1-40) 75% sample. Lines: fits of the
159 reaction kinetics, considering forward and backward reactions, Eqs. (5-7) in the main manuscript.

160

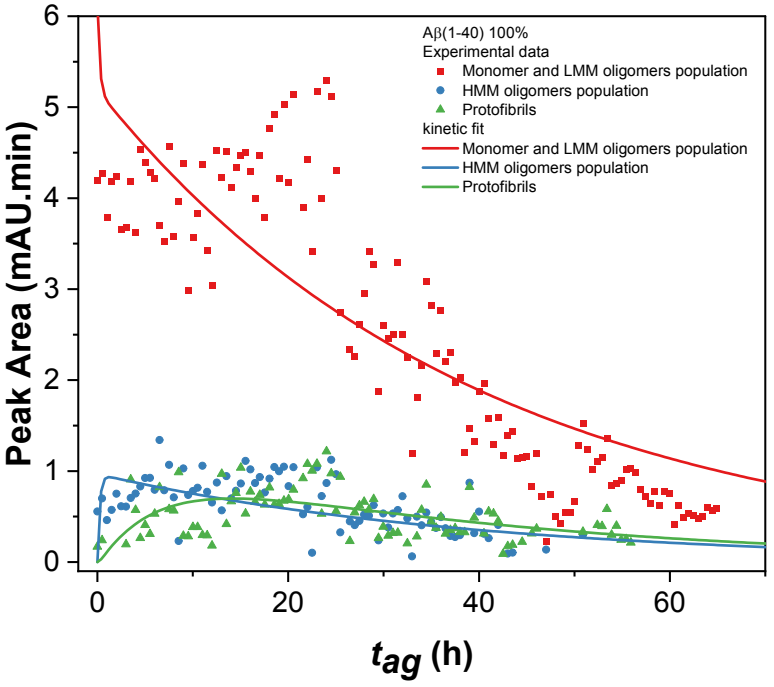

161

Figure SI.16. Symbols: time evolution of the peak area corresponding to the various populations obtained by deconvolution of the TDA signal for the Aβ(1-40) 100% sample. Lines: fits of the reaction kinetics, considering forward and backward reactions, Eqs. (5-7) in the main manuscript.

5. References

1. H. Cottet, J. P. Biron and M. Martin, On the optimization of operating conditions for Taylor dispersion analysis of mixtures, *Analyst*, 2014, **139**, 3552-3562. https://doi.org/10.1039/C4AN00192C
2. G. Taylor, Conditions under Which Dispersion of a Solute in a Stream of Solvent can be Used to Measure Molecular Diffusion, *Proc. R. Soc. London, Ser. A*, 1954, **225**, 473-477. https://doi.org/10.1098/rspa.1954.0216
3. J. Chamieh, J. Biron, L. Cipelletti and H. Cottet, Monitoring Biopolymer Degradation by Taylor Dispersion Analysis, *Biomacromolecules*, 2015, **16**, 3945-3951. https://doi.org/10.1021/acs.biomac.5b01260
4. L. Cipelletti, J.-P. Biron, M. Martin and H. Cottet, Measuring Arbitrary Diffusion Coefficient Distributions of Nano-Objects by Taylor Dispersion Analysis, *Anal. Chem.*, 2015, **87**, 8489-8496. 10.1021/acs.analchem.5b02053
5. L. Cipelletti, J.-P. Biron, M. Martin and H. Cottet, Polydispersity Analysis of Taylor Dispersion Data: The Cumulant Method, *Anal. Chem.*, 2014, **86**, 6471-6478. 10.1021/ac501115y